4896 *Chem. Mater.* **2010,** *22,* 4896–4903
DOI:10.1021/cm1006058

CHEMISTRY OF MATERIALS
Article

Liquid−Liquid Phase Separation in Model Nuclear Waste Glasses: A Solid-State Double-Resonance NMR Study

Charlotte Martineau,[†,§] Vladimir K. Michaelis,[†] Sophie Schuller,[‡] and Scott Kroeker*[,†]

[†]*Department of Chemistry, University of Manitoba, Winnipeg, Manitoba R3T 2N2, Canada,* [‡]*DEN/DTCD/SECM/LDMC, CEA Valrhô Marcoule, 30207 Bagnols-Sur-Cèze cedex, France* [§]*Current address: Tectospin, Institut Lavoisier de Versailles (ILV), UMR CNRS 8180, Université de Versailles Saint-Quentin-en-Yvelines (UVSQ), 45 Avenue des États-Unis, 78035 Versailles cedex, France*

Received February 26, 2010. Revised Manuscript Received July 21, 2010

Double-resonance nuclear magnetic resonance (NMR) techniques are used in addition to single-resonance NMR experiments to probe the degree of mixing between network-forming cations Si and B, along with the modifier cations Cs^+ and Na^+ in two molybdenum-bearing model nuclear waste glasses. The double-resonance experiments involving ^{29}Si in natural abundance are made possible by the implementation of a CPMG pulse-train during the acquisition period of the usual REDOR experiments. For the glass with lower Mo content, the NMR results show a high degree of Si−B mixing, as well as an homogeneous distribution of the cations within the borosilicate network, characteristic of a non-phase-separated glass. For the higher-Mo glass, a decrease of B−Si(Q^4) mixing is observed, indicating phase separation. ^{23}Na and ^{133}Cs NMR results show that although the Cs^+ cations, which do not seem to be influenced by the molybdenum content, are spread within the borate network, there is a clustering of the Na^+ cations, very likely around the molybdate units. The segregation of a Mo-rich region with Na^+ cations appears to shift the bulk borosilicate glass composition toward the metastable liquid−liquid immiscibility region and induce additional phase separation. Although no crystallization is observed in the present case, this liquid−liquid phase separation is likely to be the first stage of crystallization that can occur at higher Mo loadings or be driven by heat−treatment. From this study emerges a consistent picture of the nature and extent of such phase separation phenomena in Mo-bearing glasses, and demonstrates the potential of double−resonance NMR methods for the investigation of phase separation in amorphous materials.

1. Introduction

Predicting the long-term durability of nuclear waste glasses depends on reliable characterization of phase separation in these materials. Both macroscopic liquid−liquid heterogeneity and the precipitation of soluble crystalline phases can potentially degrade durability and must be well-understood. Although the use of borosilicate glasses in the immobilization of radioactive waste is a mature technology, the poor solubility of certain fission products such as molybdenum restricts waste loading in commercial glasses. Different approaches have been used to study these phenomena in alkali borosilicate glasses, like visible light scattering and electron microscopy,[1] but limited information on the phase compositions has been extracted.

Valuable information about glass composition and short-range order can be obtained by single-resonance magic angle spinning (MAS) nuclear magnetic resonance (NMR), but liquid−liquid immiscibility is very difficult to probe because of the inherent structural disorder of glasses generally producing broad overlapping peaks. Double-resonance NMR methods, however, offer the potential to probe the proximity of different nuclei.[2,3] Experiments such as rotational echo double resonance (REDOR),[4] rotational echo adiabatic passage double resonance (REAPDOR),[5] transfer of population in double resonance (TRAPDOR)[6] and cross-polarization (CP)[7] have been used to study the short- or medium-range order in alkali borate,[8,9] mixed-alkali borate,[10,11] alkali borophosphates,[12−15] and in ^{29}Si-enriched borosilicate,[16] alkali borosilicate,[17] and mixed-alkali silicate glasses.[18]

*Corresponding author. E−mail: scott_kroeker@umanitoba.ca. Fax: +12044747608.

(1) Schuller, S.; Pinet, O.; Grandjean, A.; Blisson, T. *J. Non−Cryst. Solids* **2008**, *354*, 296–300.
(2) Eckert, H.; Elbers, S.; Epping, J. D.; Janssen, M.; Kalwei, M.; Strojek, W.; Voigt, U. *Top. Curr. Chem.* **2004**, *246*, 195–233.
(3) Gullion, T.; Vega, A. *Prog. Nucl. Magn. Reson. Spectrosc.* **2005**, *47*, 123–136.
(4) Gullion, T.; Schaefer, J. *J. Magn. Reson.* **1989**, *81*, 196–200.
(5) Gullion, T. *J. Magn. Reson.* **1995**, *117*, 326–329.
(6) Grey, C. P.; Vega, A. J. *J. Am. Chem. Soc.* **1995**, *117*, 8232–8242.
(7) Schaefer, J.; Stejskal, E. O. *J. Am. Chem. Soc.* **1976**, *98*, 1031–1032.
(8) Janssen, M.; Eckert, H. *Solid State Ionics* **2000**, *136−137*, 1007–1014.
(9) Aguiar, P. M.; Kroeker, S. *Solid State Nucl. Magn. Reson.* **2005**, *27*, 10–15.
(10) Voigt, U.; Lammert, H.; Eckert, H.; Heuer, A. *Phys. Rev. B* **2005**, *72*, 064207.
(11) Epping, J. D.; Eckert, H.; Imre, Á. W.; Mehrer, H. *J. Non−Cryst. Solids* **2005**, *351*, 3521–3529.
(12) Zeyer−Düsterer, M.; Montagne, L.; Palavit, G.; Jäger, C. *Solid State Nucl. Magn. Reson.* **2005**, *27*, 50–64.

 Published on Web 08/05/2010

Table 1. Analyzed Chemical Compositions (mol %) of the Glasses Under Study

name	B_2O_3	SiO_2	Na_2O	Cs_2O	MoO_3
Mo-0.8	17.6	63.6	16.4	1.6	0.8
Mo-1.7	16.7	61.6	18.1	2.0	1.7

The aim of this paper is to show that the spatial proximities between atoms extracted from these double-resonance NMR experiments can also be advantageously used to investigate amorphous heterogeneity resulting from liquid−liquid phase separation phenomena in the melt. Our study focuses on two non-radioactive simplified mixed-alkali borosilicate glasses, the compositions of which derive from the industrial French nuclear waste glass "R7T7". The glass was designed by keeping the same oxides ratio as in the complex glass for SiO_2, B_2O_3, Na_2O, and enriching in Cs_2O. One glass contains 0.8 mol % MoO_3 (Mo-0.8) and is known to be homogeneous according to high-resolution transmission electron microscopy (HRTEM) data,[19] whereas the second glass contains 1.7 mol % (Mo-1.7) and was found to be phase-separated.[19] Single-resonance NMR data are presented, with a particular emphasis on the use of the Carr−Purcell−Meiboom−Gill[20,21] (CPMG) NMR experiment to detect the low-natural-abundance silicon-29 nuclide. Various double-resonance NMR techniques are used to probe the degree of mixing of network-forming atoms Si and B, along with the modifier cations Cs^+ and Na^+ in these glasses. The effective use of double-resonance NMR methods involving naturally abundant ^{29}Si is made possible by the implementation of a CPMG pulse-train in the acquisition period of the RE-DOR experiment. The overall results present a consistent picture of the nature and extent of the liquid−liquid phase separation processes occurring in Mo-1.7, and demonstrate the potential of such methods for the study of phase separation in amorphous materials.

2. Material and Methods

2.1. Glass Preparation. Glasses (100 g batches) were prepared by melting reagent grade SiO_2, H_3BO_3, Na_2CO_3, $CsNO_3$, and MoO_3 powders at 1300 °C for 3 h in platinum crucibles under air and quenching onto a metal plate (cooling of about 10^3°C/min). The names and compositions of the glasses are given in Table 1. Compositions were analyzed by electron probe microanalysis (EPMA) using a SX100 Cameca instrument with an accelerating voltage of 12 kV, a beam current of 10 nA, and a defocused beam to reduce sodium migration.[22] Boron was analyzed directly using a boracite standard and LPC3 crystal spectrometer.[23] Slight compositional variations are likely due to elemental volatility at the high melting temperature.[24] Optical microscopy and powder X-ray diffraction revealed no evidence of crystallinity.

2.2. NMR Experiments. NMR experiments were conducted on a Varian ^{UNITY}INOVA 600 spectrometer (B_0 = 14.1 T), using 3.2 mm double-resonance or triple-resonance probes that are free of boron background signals. At this magnetic field, the Larmor frequencies of ^{11}B, ^{23}Na, ^{29}Si, ^{133}Cs, and ^{95}Mo are 192.40, 158.64, 119.15, 79.67, and 39.08 MHz, respectively. Quantitative ^{11}B (I = 3/2, N. A. = 80.1%) single pulse MAS (8 kHz) NMR spectra were recorded using a short pulse length (0.5 μs, 18° tip angle) and recycle delays of 5 s. ^{29}Si (I = 1/2, N. A. = 4.7%) MAS (10 kHz) CPMG[20,21] spectra were recorded for the two glasses using 3 μs 90° pulses and 190 s recycle delays. For the CPMG experiment, the delay between the echoes was set to 4 ms (spikelet separation of 250 Hz in the NMR spectrum), and 64 echoes were collected; 256 and 64 transients were accumulated for the Hahn−echo and the CPMG spectra, respectively. The ^{23}Na (I = 3/2, N. A. = 100%) MAS (10 kHz) spectra were acquired using a short pulse length (0.5 μs) and 2 s recycle delays. 6144 transients were accumulated. The ^{133}Cs (I = 7/2, N. A. = 100%) and ^{95}Mo (I = 5/2, N. A. = 15.9%) MAS (20 kHz) Hahn-echoes respectively employed 3 and 1.7 μs 90° pulses, recycle delays of 60 and 10 s, and accumulations of 128 and 33744 (~4 days) transients. ^{11}B, ^{29}Si, ^{23}Na, ^{133}Cs and ^{95}Mo chemical shifts were referenced to 0.1 M H_3BO_3 (19.6 ppm), 3-(trimethylsilyl)-propanesulfonic (1.43 ppm), 1 M NaCl (0 ppm), 0.5 M CsCl (0 ppm), and 2 M Na_2MoO_4 (0 ppm), respectively. ^{23}Na and ^{133}Cs static (i.e., non−spinning) Hahn−echo spectra NMR spectra were recorded at room temperature, with variable interpulse delays; 128 and 256 transients were accumulated for ^{23}Na and ^{133}Cs, respectively. The NMR spectra were processed using the Dmfit software.[25]

Double-resonance NMR spectra were acquired using a triple−resonance 3.2 mm probe doubly−tuned to the corresponding Larmor frequencies. The $^{11}B\{^{133}Cs,^{23}Na\}$ REDOR[26] experiments were recorded at a MAS frequency of 6250(1) Hz. The lengths of the ^{133}Cs (7 μs) and ^{23}Na (10 μs) dephasing 180° pulses were adjusted for each nucleus to obtain the maximum signal loss for a given dephasing time. A separate nutation NMR experiment showed that these conditions correspond to selective excitation of the central $1/2 \leftrightarrow -1/2$ transition of ^{23}Na. The $^{29}Si\{^{11}B,^{133}Cs\}$ REDOR−CPMG experiments were recorded at a MAS frequency of 6250 Hz using the pulse sequence depicted in Figure 1. The CPMG block used 2 ms delays between the echoes. Sixteen to 32 transients (50 to 100 min per spectrum) were accumulated for each recoupling time. $^{29}Si\{^{11}B\}$ CP−CPMG[27] spectra were recorded at an MAS frequency of 10 kHz. The Hartmann−Hahn match (using a radiofrequency field for ^{11}B corresponding to a nutation frequency of ~42 kHz) and contact time (4 ms) were optimized on datolite,[28] which contains one four-coordinate boron and one silicon site. The recycle delays were set to that of ^{11}B and 1536 transients were collected.

(13) Strojek, W.; Kalwei, M.; Eckert, H. *J. Phys. Chem. B* **2004**, *108*, 7061–7073.
(14) Strojek, W.; Fehse, C. M.; Eckert, H.; Ewald, B.; Kniep, R. *Solid State Nucl. Magn. Reson.* **2007**, *32*, 89–98.
(15) Raskar, D. B.; Eckert, H.; Ewald, B.; Kniep, R. *Solid State Nucl. Magn. Reson.* **2008**, *34*, 20–31.
(16) Van Wüllen, L.; Schwering, G. *Solid State Nucl. Magn. Reson.* **2002**, *21*, 134–144.
(17) Muñoz, F.; Montagne, L.; Delevoye, L.; Durán, A.; Pascual, L.; Cristol, S.; Paul, J.-F. *J. Non-Cryst. Solids* **2006**, *352*, 2958–2968.
(18) Gee, B.; Eckert, H. *J. Phys. Chem.* **1996**, *100*, 3705–3712.
(19) Kroeker, S.; Schuller, S.; Farnan, I. **2010**, in preparation.
(20) Carr, H. Y.; Purcell, E. M. *Phys. Rev.* **1954**, *94*, 630–638.
(21) Meiboom, S.; Gill, D. *Rev. Sci. Instrum.* **1958**, *29*, 688–691.
(22) Morgan, VI, G. B.; London, D. *Am. Mineral.* **2005**, *90*, 1131–1138.
(23) Bastin, G. F.; Heijligers, J. M. *Microchim. Acta* **1992**, *12*, 19–36.
(24) Michaelis, V. K.; Kroeker, S. *Phys. Chem. Glasses: Eur. J. Glass Sci. Technol., B* **2009**, *50*, 249–252.
(25) Massiot, D.; Fayon, F.; Capron, M.; King, I.; Le Calvé, S.; Alonso, B.; Durand, J. O.; Bujoli, B.; Gan, Z.; Hoatson, G. *Magn. Reson. Chem.* **2002**, *40*, 70–76.
(26) Garbow, J. R.; Gullion, T. *J. Magn. Reson.* **1991**, *95*, 442–445.
(27) Lipton, A. S.; Sears, J. A.; Ellis, P. D. *J. Magn. Reson.* **2001**, *151*, 48–59.
(28) Foit, F. F.; Phillips, M. W.; Gibbs, G. V. *Am. Mineral.* **1973**, *58*, 909–914.

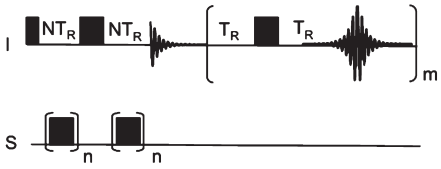

Figure 1. Pulse sequence for the REDOR−CPMG experiment. *I* denotes the ^{29}Si nucleus, whereas *S* denotes either the ^{11}B, ^{23}Na, or ^{133}Cs nuclei. T_R and NT_R represent rotor-synchronized delays.

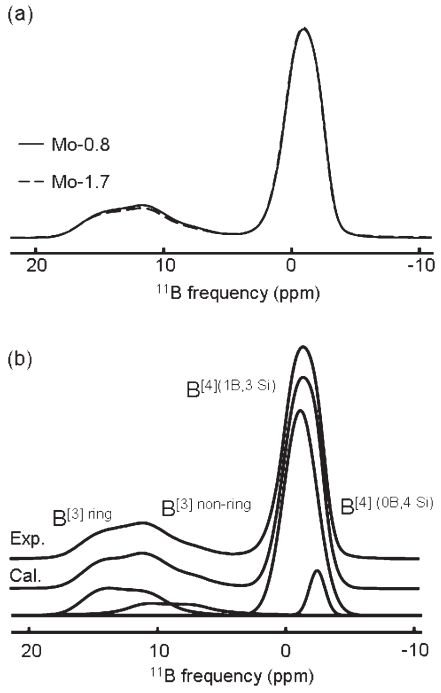

Figure 2. (a) Experimental ^{11}B MAS NMR spectra of the two borosilicate glasses under study. (b) Experimental and calculated ^{11}B MAS (8 kHz) NMR spectrum of the Mo-0.8 glass. The individual contributions are shown.

The CPMG block used the same parameters as the ^{29}Si CPMG described above.

2.3. Quantum Chemical Calculations. Borosilicate model clusters designed to mimic the glass local structure ($CsSiB_3O_{10}H_6$, $CsSiB_3O_{13}H_9$, $CsSi_6B_7O_{34}H_{19}$), were constructed using GaussView 3.09 and optimized with Gaussian03,[29] supported on a SUN X4440 server with 16 cores and 64 GB RAM. Calculations consisted of a complete optimization using LSDA[30−32] and B3LYP[33−35] hybrid-density functional theory using the LanL2-DZ[36−39] basis set.

3. Results and Discussion

3.1. Single-Resonance NMR Experiments. *^{11}B MAS NMR.* The ^{11}B MAS NMR spectra of the two glasses under study are displayed in Figure 2a. The spectra show two contributions, well resolved at the magnetic field employed (14.1 T). The major peak centered around −1 ppm corresponds to four-fold coordinated boron atoms ($B^{[4]}$, BO_4), whereas the less-prominent peak centered around 12 ppm corresponds to three-fold coordinated boron atoms ($B^{[3]}$, BO_3). As the two ^{11}B resonances have significantly different nutation rates because of their very different C_Q values, the quantitative nature of the NMR spectra was ensured by using small flip angles (about 18°). The populations of each boron site (70% of $B^{[4]}$ and 30% of $B^{[3]}$ for Mo-0.8 and 73% of $B^{[4]}$ and 27% of $B^{[3]}$ for Mo-1.7) were determined by integration of the central transitions and corrected to take into account the different C_Q values.[40] A small increase of the $B^{[4]}/B^{[3]}$ ratio is observed for the higher Mo-content glass, which can be attributed to the slightly higher alkali (Cs + Na) content in Mo-1.7.

The ^{11}B NMR line shapes are complex and neither $B^{[3]}$ or $B^{[4]}$ can be described by a single quadrupolar peak shape or Gaussian line, suggesting the presence of more than one type of boron for each coordination environment (Figure 2b). The small quadrupolar coupling constant (C_Q) for $B^{[4]}$ (440 kHz) was estimated by reconstruction of the spinning sideband manifold (not shown). The isotropic chemical shift (δ_{iso}) of the two $B^{[4]}$ units are −1 and −2 ppm, characteristic of boron atoms with (1 B, 3 Si) and (0 B, 4 Si) neighbors, respectively.[41,42] The quadrupolar parameters for the two BO_3 sites are similar and were estimated by reconstruction of the central transitions ($C_Q \approx 2.5$ MHz, $\eta = 0$ for both). The two $B^{[3]}$ components, with δ_{iso} of 17 and 13 ppm, can be assigned to boron in some sort of ring structure, and to boron atoms in non-ring sites, respectively.[41,42] There is no evidence for the presence of nonbridging oxygen atoms (NBOs) on the BO_3 units. Although these fits may not be unique, they utilize well-known parameters and structures known to be present in these types of glasses.[43,44]

(29) Frisch, M. J.; Trucks, G. W.; Schlegel, H. B.; Scuseria, G. E.; Robb, M. A.; Cheeseman, J. R.; Montgomery, Jr., J. A.; Vreven, T.; Kudin, K. N.; Burant, J. C.; Millam, J. M.; Iyengar, S. S.; Tomasi, J.; Barone, V.; Mennucci, B.; Cossi, M.; Scalmani, G.; Rega, N.; Petersson, G. A.; Nakatsuji, H.; Hada, M.; Ehara, M.; Toyota, K.; Fukuda, R.; Hasegawa, J.; Ishida, M.; Nakajima, T.; Honda, Y.; Kitao, O.; Nakai, H.; Klene, M.; Li, X.; Knox, J. E.; Hratchian, H. P.; Cross, J. B.; Bakken, V.; Adamo, C.; Jaramillo, J.; Gomperts, R.; Stratmann, R. E.; Yazyev, O.; Austin, A. J.; Cammi, R.; Pomelli, C.; Ochterski, J. W.; Ayala, P. Y.; Morokuma, K.; Voth, G. A.; Salvador, P.; Dannenberg, J. J.; Zakrzewski, V. G.; Dapprich, S.; Daniels, A. D.; Strain, M. C.; Farkas, O.; Malick, D. K.; Rabuck, A. D.; Raghavachari, K.; Foresman, J. B.; Ortiz, J. V.; Cui, Q.; Baboul, A. G.; Clifford, S.; Cioslowski, J.; Stefanov, B. B.; Liu, G.; Liashenko, A.; Piskorz, P.; Komaromi, I.; Martin, R. L.; Fox, D. J.; Keith, T.; Al−Laham, M. A.; Peng, C. Y.; Nanayakkara, A.; Challacombe, M.; Gill, P. M. W.; Johnson, B.; Chen, W.; Wong, M. W.; Gonzalez, C.; Pople, J. A. *Gaussian 03, Revision C.02*; Gaussian, Inc.: Wallingford, CT, 2004.
(30) Hohenberg, P.; Kohn, W. *Phys. Rev.* **1964**, *136*, B864–871.
(31) Kohn, W.; Sham, L. J. *Phys. Rev.* **1965**, *140*, A1133–1138.
(32) Vosko, S. H.; Wilk, L.; Nusair, M. *Can. J. Phys.* **1980**, *58*, 1200–1211.
(33) Becke, A. D. *J. Chem. Phys.* **1993**, *98*, 5648.
(34) Lee, C.; Yang, W.; Parr, R. G. *Phys. Rev. B: Condens. Matter* **1988**, *37*, 785.
(35) Miehlich, B.; Savin, A.; Stoll, H.; Preuss, H. *Chem. Phys. Lett.* **1989**, *157*, 200–206.
(36) Dunning, T. H.; Hay, P. J. *Mod. Theor. Chem.* **1976**, *3*, 1–28.
(37) Hay, P. J.; Wadt, W. R. *J. Chem. Phys.* **1985**, *82*, 270–283.
(38) Wadt, W. R.; Hay, P. J. *J. Chem. Phys.* **1985**, *82*, 284–298.
(39) Woon, D. E.; Dunning, T. H., Jr. *J. Chem. Phys.* **1993**, *98*, 1358–1371.
(40) Massiot, D.; Bessada, C.; Coutures, J.-P.; Taulelle, F. *J. Magn. Reson.* **1990**, *90*, 231–242.
(41) Du, L.-S.; Stebbins, J. F. *J. Non-Cryst. Solids* **2003**, *315*, 239–255.
(42) Du, L.-S.; Stebbins, J. F. *Chem. Mater.* **2003**, *15*, 3913–3921.
(43) Kroeker, S.; Stebbins, J. F. *Inorg. Chem.* **2001**, *40*, 6239–6246.
(44) Parkinson, B. G.; Holland, D.; Smith, M. E.; Howes, A. P.; Scales, C. R. *J. Phys.: Condens. Matter* **2007**, *19*, 415114.

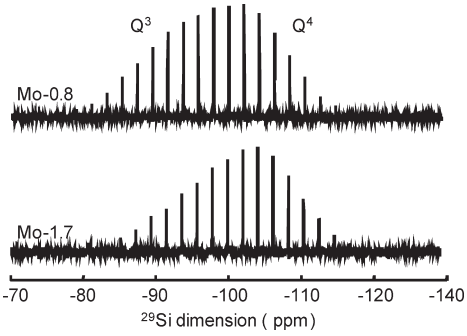

Figure 3. ^{29}Si MAS (10 kHz) CPMG spectra of the two borosilicate glasses under study.

^{29}Si MAS NMR. Because of the low natural abundance of ^{29}Si (4.7%) and long spin−lattice relaxation time T_1 (~35 s in the glasses under study), direct observation of silicon-29 using a Hahn−echo requires a particularly long experimental time (about 13 h for our glasses). It has been shown that enhancement of the ^{29}Si NMR sensitivity can be obtained[45,46] using the CPMG experiment.[20,21] The ^{29}Si CPMG NMR spectra of the two studied borosilicate glasses (Figure 3) show evidence for the presence of Q^4 ($\delta_{iso} < -100$ ppm), Q^3 (δ_{iso} between −100 and −90 ppm) and possibly of Q^2 (δ_{iso} between −95 and −80 ppm) species, where Q^n represents Si atoms surrounded by n bridging oxygen atoms.[47] Because of the lack of resolution, it is difficult to determine the proportion of each Q^n. However, the $Q^{2/3}/Q^4$ ratio in Mo-1.7 is noticeably lower than that in the Mo-0.8 glass.

Charge balance arguments can be used to assess the likelihood of different Q^n species being present in the glasses. The anionic charges of BO_4^- and Si Q^3 and Q^2 must be compensated by the positive charges of the Na^+ and Cs^+ cations, the numbers of which are known from the glass composition. The number of BO_4^- can be calculated from the glass composition (Table 1) and the $B^{[4]}/B^{[3]}$ measured from ^{11}B MAS NMR. Molybdenum, incorporated as "isolated" MoO_4^{2-} units in alkali−rich regions and not directly linked to the silicate or borosilicate network,[48,49] are also accounted for in the calculation. The number of (negatively charged) nonbridging oxygens on BO_3 is negligible, judging from ^{11}B MAS NMR and by studies of glasses of similar compositions.[41,50] This allows us to predict the maximum number of negative charges remaining on Si units to be 15 and 20%, suggesting that little to no Q^2 is expected to be present in these glasses.

^{95}Mo, ^{23}Na, and ^{133}Cs MAS NMR. Because of the low natural abundance of ^{95}Mo (15.7%), its low magnetogyric ratio, γ (1.751×10^7 rad T^{-1} s^{-1}), the low amount of MoO_3 in the glasses (< 2%), and long recycle delays (10 s),

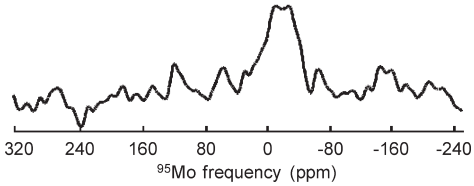

Figure 4. ^{95}Mo MAS (20 kHz) NMR spectrum of the Mo-1.7 glass.

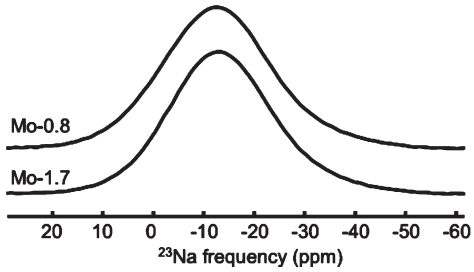

Figure 5. Central transitions of the ^{23}Na MAS (10 kHz) NMR spectra of the two borosilicate glasses under study.

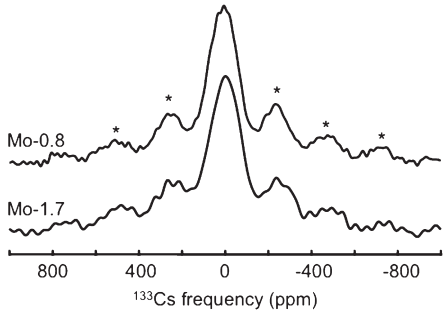

Figure 6. ^{133}Cs MAS (20 kHz) NMR spectra of the two borosilicate glasses under study. Stars indicate the positions of spinning sidebands.

the signal-to-noise ratio of the ^{95}Mo MAS NMR spectrum (Figure 4) of the Mo-1.7 glass is poor despite four days of accumulation. The spectrum shows a single broad resonance ($C_Q \approx 2.3$ MHz) with $\delta_{iso} \approx 7$ ppm, characteristic of molybdenum in four-fold coordination.[51−54] ^{95}Mo NMR, however, is not sensitive to the type of alkali neighbors,[54] so no further information concerning the Mo environment can be deduced from the NMR spectrum.

The ^{23}Na MAS NMR spectra of the two glasses (Figure 5) are almost indistinguishable and show a single broad resonance ($C_Q \approx 3$ MHz and $\delta_{iso} \approx -6$ (± 2) ppm), characteristic of the disordered environments (bond length and angle) around the Na^+ cations. Likewise, ^{133}Cs MAS NMR spectra of the two glasses (Figure 6) show a single broad resonance centered around 10 (± 20) ppm flanked by spinning sidebands. Because of the small quadrupole moment of ^{133}Cs,[55] the widths of the resonances (~200

(45) Larsen, F. H.; Farnan, I. *Chem. Phys. Lett.* **2002**, *357*, 403–408.
(46) Wiench, J. W.; Lin, V. S.-Y.; Pruski, M. *J. Magn. Reson.* **2008**, *193*, 233–242.
(47) MacKenzie, K. J. D.; Smith, M. E. *Multinuclear Solid−State NMR of Inorganic Materials*; Pergamon: Amsterdam, 2002.
(48) Calas, G.; Le Grand, M.; Galoisy, L.; Ghaleb, D. *J. Nucl. Mater.* **2003**, *322*, 15–20.
(49) Farges, F.; Siewert, R.; Brown, G. E., Jr.; Guesdon, A.; Morin, G. *Can. Mineral.* **2006**, *44*, 731–753.
(50) Dell, W. J.; Bray, P. J.; Xiao, S. Z. *J. Non-Cryst. Solids* **1983**, *58*, 1–16.
(51) Edwards, J. C.; Adams, R. D.; Ellis, P. D. *J. Am. Chem. Soc.* **1990**, *112*, 8349–8364.
(52) Machidal, N.; Eckert, H. *Solid State Ionics* **1998**, *107*, 255–268.
(53) Santagneli, S. H.; de Araujo, C. C.; Strojek, W.; Eckert, H.; Poirier, G.; Ribeiro, S. J. L.; Messaddeq, Y. *J. Phys. Chem. B* **2007**, *111*, 10109–10117.
(54) Kroeker, S.; Farnan, I.; Schuller, S.; Advocat, T. *Mater. Res. Soc. Symp. Proc.* **2009**, *1124*, Q03–06.
(55) Pernpointner, M.; Schwerdtferger, P.; Hess, B. A. *J. Chem. Phys.* **1998**, *108*, 6739–6747.

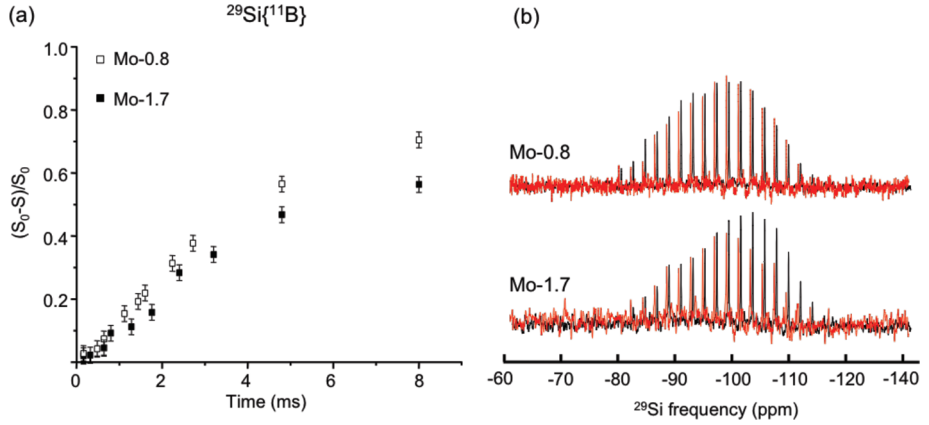

Figure 7. (a) ^{29}Si{^{11}B} REDOR−CPMG curves and (b) ^{29}Si{^{11}B} CP−CPMG MAS (10 kHz) NMR spectra (red) compared with the ^{29}Si CPMG spectra (black), slightly offset for comparison purposes, of the two borosilicate glasses under study.

ppm) are mainly due to chemical shift distributions, reflecting the distribution of environments around the Cs^+ cations.[56]

The multinuclear single-resonance NMR data are all characteristic of disordered environments. In particular, ^{133}Cs, ^{23}Na, and ^{95}Mo MAS NMR are sensitive to the presence of crystalline inclusions, revealing sharp peaks superimposed upon broad featureless peaks from the glassy components.[57] Hence, devitrification can be ruled out. However, the lack of resolution of the glassy 1D NMR spectra prevents any further discussion regarding the type or degree of glass-in-glass homogeneity in these materials. Therefore, additional details were sought by double-resonance NMR experiments.

3.2. Network-Former Mixing. Double-resonance REDOR-type experiments are based on heteronuclear dipolar interactions, and therefore the NMR response in these experiments depends on internuclear distances. Although these glasses are too complex for accurate distance measurements, REDOR experiments can provide qualitative information about internuclear proximities, and hence network mixing. The REDOR curves are generated by plotting the normalized difference of intensity between a reference echo spectrum and a spectrum recorded with reintroduction of dipolar interactions, for a series of recoupling times.[3] In the case of the ^{29}Si−^{11}B spin pair (with ^{29}Si in natural abundance), the double-resonance experiments are challenging. On one hand, the ^{11}B{^{29}Si} REDOR experiment (i.e., recording ^{11}B, dephasing ^{29}Si) is not very sensitive because of the low natural abundance of ^{29}Si. On the other hand, building a ^{29}Si{^{11}B} REDOR curve (i.e., recording ^{29}Si, dephasing ^{11}B) requires long experimental time, because each ^{29}Si echo takes more than 13 hours of accumulation. It has been shown that a CPMG[20,21] train of π pulses can be implemented within the acquisition period of usual NMR experiments, like CP,[27] heteronuclear correlation (HETCOR),[58] or double-quantum single-quantum (DQ−SQ)[46,59] experiments, allowing acquisition of natural abundance ^{29}Si high-resolution NMR spectra in reduced experimental time. Accordingly, we have implemented the CPMG pulse train during the acquisition of the echo spectra of the REDOR experiment to measure the ^{29}Si{^{11}B} dephasing curves in our glasses (Figure 7). Like a REDOR curve, a REDOR−CPMG curve is generated by measuring the difference between a CPMG reference spectrum and a CPMG spectrum recorded with 180° pulses on the second nucleus, for different dephasing times. These ^{29}Si{^{11}B} double-resonance experiments involve the application of 180° recoupling pulses on the spin-3/2 ^{11}B nuclei. In this case, the REDOR response is subject to the efficiency of the recoupling of the outer $|\pm 3/2\rangle$ Zeeman state.[13] Four-coordinated boron sites have a rather small C_Q (440 kHz) that allows for efficient recoupling. By contrast, the larger C_Q value (~2.5 MHz) of the three−coordinate boron attenuates the REDOR response under the same experimental conditions.[13] Moreover, as mentioned above, the nutation rates of $B^{[3]}$ and $B^{[4]}$ are very different and isolated spin pairs are unlikely to be present in these systems. For these reasons, it is not possible to extract quantitative data from the curves. However, because the proportion of $B^{[3]}$ and $B^{[4]}$, as well as their respective C_Q values, are similar in the two glasses, results can still be directly compared to obtain qualitative information.

The ^{29}Si{^{11}B} double-resonance curves for the two borosilicate glasses are presented in Figure 7a. As the ^{29}Si resonances corresponding to the Q^3 and Q^4 units are not resolved in the NMR spectra, the curves show the overall REDOR response of all silicon species. A nonzero dipolar interaction between Si and B is observed, indicating that both glasses have appreciable mixing between silicon and boron network formers. However, the non-phase-separated Mo-0.8 glass shows the strongest dipolar fields, implying the greatest degree of network mixing. The phase-separated Mo-1.7 glass shows a significantly lower dephasing plateau, suggestive of some fraction of silicon atoms far from boron-11 nuclei, possibly

(56) Michaelis, V. K.; Aguiar, P. M.; Kroeker, S. *J. Non-Cryst. Solids* **2007**, *353*, 2582–2590.
(57) Kroeker, S.; Higman, C. S.; Michaelis, V. K.; Svenda, N. B.; Schuller, S. *Mater. Res. Soc. Symp. Proc.* **2010**, accepted.
(58) Kennedy, G. J.; Wiench, J. W.; Pruski, M. *Solid State Nucl. Magn. Reson.* **2008**, *33*, 76–81.
(59) Goswami, M.; Madhu, P. K.; Dittmer, J.; Nielsen, N. C.; Ganapathy, S. *Chem. Phys. Lett.* **2009**, *478*, 287–291.

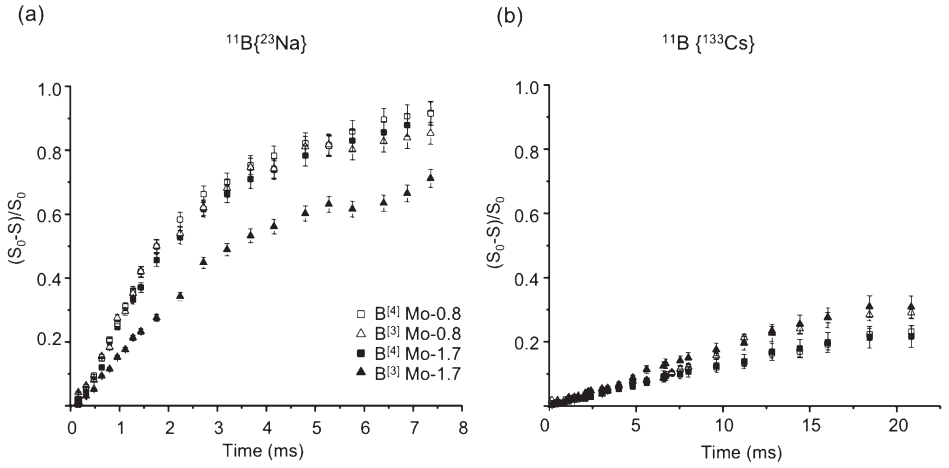

Figure 8. (a) ^{11}B{^{23}Na} and (b) ^{11}B{^{133}Cs} REDOR curves of the two borosilicate glasses under study.

in a phase-separated region. Accounting for the poorer recoupling efficiency of BO_3 relative to BO_4 units, the data may also be explained by Si atoms in a region depleted of BO_4 units and principally surrounded by BO_3 units. Both explanations imply two compositionally distinct amorphous regions.

To obtain species-specific details on the Si−B proximities, ^{29}Si{^{11}B} CP−CPMG[27] MAS spectra were recorded (Figure 7b). For the Mo-0.8 glass, the overall shapes of the CPMG and CP−CPMG spectra are essentially identical, indicating homogeneous mixing between Si and B. In contrast, the CP−CPMG spectrum of the Mo-1.7 glass exhibits a decrease in the relative intensity of the Si Q^4 region (Figure 7b). Because both ^{11}B{^{29}Si} CP−CPMG spectra were recorded under similar conditions, this very likely indicates that some silicon atoms are not linked to boron atoms and are segregated in a Si-Q^4-rich region in the Mo-1.7 glass. This observation is consistent with the lower recoupling observed in the REDOR−CPMG experiment on this glass (Figure 7a).

Because of the spin dynamics involved in the spin-locking and cross-polarization process, magnetization transfer from quadrupolar nuclei with large C_Q values is efficient if the parameter $\alpha = \nu_{RF}{}^2/(\nu_{MAS} \times \nu_Q)$ is much lower than 1,[60] where ν_{RF} is the radiofrequency field for the quadrupolar nucleus, ν_{MAS} the MAS frequency, and ν_Q the quadrupolar frequency. In our study, the experiments were optimized to transfer polarization from four−coordinate ^{11}B to ^{29}Si (i.e., $\nu_{RF}(^{11}B)$ = 42 kHz, ν_{MAS} = 10 kHz, see experimental section), thus, for $^{11}B^{[3]}$ $\alpha \approx$ 0.14, still allowing some magnetization to be transferred from $B^{[3]}$ to ^{29}Si. $B^{[3]}$ and $B^{[4]}$ atoms have distinct nutation rates and therefore, if the first pulse of the CP-CPMG experiment was set to correspond to a 90° tip angle for $^{11}B^{[4]}$, it corresponds to a lower tip angle (~45°) for $^{11}B^{[3]}$. Therefore, the transfer from $^{11}B^{[3]}$ to ^{29}Si is expected to be much less efficient, but not negligible. This inefficiency demands that we admit the subtly different explanation that some fraction of Si-Q^4 units in the Mo-1.7 glass are located in a region low in BO_4 units. Because of the sparseness of BO_3 species in the bulk glass, the poor magnetization transfer efficiency and the possibility of weak longer-range dephasing effects, there remains some uncertainty in the location of BO_3 and BO_4 units with respect to Si-Q^4 units.

3.3. Alkali Cation Partitioning. Double-resonance NMR experiments between formers (Si,B) and modifiers (Na,Cs) as well as ^{23}Na and ^{133}Cs static echo experiments were also employed to probe the alkali cation partitioning within the glassy network.

(^{11}B,^{29}Si){^{23}Na,^{133}Cs} Double-Resonance NMR Experiments. The ^{11}B{^{23}Na} REDOR curves of the two glasses are presented in Figure 8a. Because the recoupling pulses are applied on the quadrupolar nucleus ^{23}Na, the recoupling efficiency depends on the values of C_Q.[13] However, the ^{23}Na C_Q values are similar in the two glasses under study, so the curves can be directly compared for qualitative conclusions. Because the four- and three-coordinated boron sites have significantly different nutation rates, two sets of ^{11}B{^{23}Na} experiments were run separately, using pulse lengths optimized on each of the resonances. In the two glasses, the $^{11}B^{[4]}${^{23}Na} REDOR curves show a very fast recoupling, indicating that the negative charge on BO_4^- is balanced by sodium cations. Such strong $^{11}B^{[4]}${^{23}Na} dipolar fields have been previously observed in sodium borate glasses,[8] and are characteristic of a homogeneous distribution of the Na^+ cations within the glassy borate network. In such cases, similar dipolar fields are measured between $B^{[3]}$−Na and $B^{[4]}$−Na, indicating a homogeneous distribution of the Na^+ cations throughout the glassy matrix, as seen here for Mo-0.8. Moreover, because of the high Na content in these two glasses (16.4 and 18.1 mol %), both $B^{[3]}$ and $B^{[4]}$ are likely to have Na^+ cations in their vicinity. In contrast, the $^{11}B^{[3]}${^{23}Na} dipolar field in the phase-separated Mo-1.7 glass is significantly lower than that of $^{11}B^{[4]}${^{23}Na}, indicating either that $B^{[3]}$-Na average distances are longer than those of $B^{[4]}$-Na, or that there are fewer of them. This observation is consistent with the segregation of BO_3 units into a Si-Q^4-rich phase, as suggested by the ^{11}B{^{29}Si} double-resonance NMR experiments, where the elevated levels of (neutral) Q^4 species results in reduced levels of network modifying cations.

(60) Vega, A. J. *Solid State Nucl. Magn. Reson.* **1992**, *1*, 17–32.

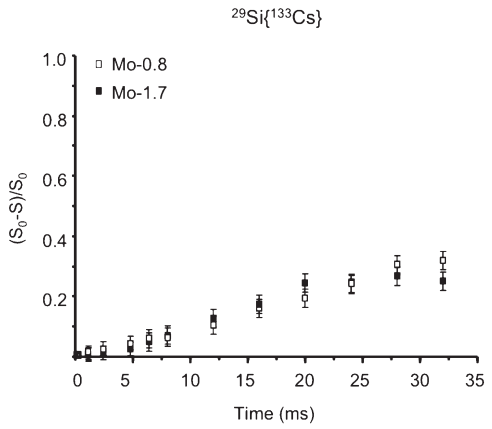

Figure 9. ^{29}Si{^{133}Cs} REDOR−CPMG curves of the two borosilicate glasses under study.

The ^{29}Si{^{23}Na} REDOR−CPMG spectra are too noisy to get reliable data on Si−Na proximities. However, considering the proportion of Na^+ cations in the glasses, the negative charges of Q^3 and Q^2 are expected to be jointly charge−compensated by Na^+ and Cs^+ cations.

The ^{11}B{^{133}Cs} REDOR and ^{29}Si{^{133}Cs} REDOR−CPMG curves of the two glasses are presented in Figures 8b and 9, respectively. Because the ^{133}Cs nucleus has a very small quadrupolar moment (and correspondingly small C_Q values), the REDOR response is expected to be efficient. All dephasing curves are similar with a maximum plateau of 30% reached at relatively long recoupling time of about 20 ms, indicating small and similar ^{133}Cs dipolar fields for both network-forming cations. While the low plateau may be understood in terms of the small amount of Cs in the glasses (1.6 and 2.0 mol %), the strong similarity between the Si and B curves implies that the Si−Cs distances are shorter (or more plentiful) than the B−Cs distances, because the magnetogyric ratio of ^{29}Si is nearly 40% lower than that of ^{11}B. As such, it appears that Cs^+ cations preferentially act as network modifiers for the Si Q^3s rather than as charge compensators for $B^{[4]}$.

Although this conclusion is supported by the low degree of BO_4^- dephasing by ^{133}Cs, the consistently larger net ^{133}Cs dipolar field at BO_3 is initially surprising. A similar observation has been rationalized in high-alkali binary cesium-borate glasses by the network-modifying capacity of Cs^+ to form nonbridging oxygens on BO_3.[9] However, no evidence of nonbridging oxygens on boron can be found in these more complex multicomponent glasses. In the present case, it appears instead to be due to secondary effects, where the BO_3 experiences the dipolar field of the Cs^+ associated with neighboring Si-Q^3s. The plausibility of this explanation was assessed both by ab initio geometry optimizations[29] of model clusters containing $B^{[3]}$−O−Si−$O^-\cdots Cs^+$ and $B^{[4]}$−O−Si−$O^-\cdots Cs^+$, and by comparisons with typical Cs−B distances in minerals. Both approaches yield larger $B^{[4]}$−Cs^+ distances than $B^{[3]}$−Cs^+ (~4.8 Å for Cs−$B^{[3]}$ and ~5.5 Å for Cs−$B^{[4]}$), confirming that charge repulsion may be responsible for this seemingly paradoxical result.

^{23}Na and ^{133}Cs Static Echo. It has been shown that spin−echo decays in nonspinning samples can yield valuable information about homonuclear dipolar couplings.[61,62] These experiments were used to probe the extent of Cs−Cs and Na−Na proximities in the glasses. The ^{133}Cs and ^{23}Na spin−echo decays of the two glasses are presented in Figure 10. Because the quadrupolar nature of the nuclei can interfere with a quantitative treatment of the dipolar second moment, and because the experiments were recorded at room temperature where cationic motion can influence the dipolar fields, the comparative evolution of the ^{133}Cs and ^{23}Na curves are discussed qualitatively. The trend in the ^{133}Cs spin−echo decay (Figure 10a) is similar, within experimental error, for the two glasses. Because no Cs^+ clustering is expected in the non-phase-separated Mo-0.8 glass, by analogy, it can be inferred that no Cs^+ clustering around the Mo ions occurs in the Mo-1.7 glass. By contrast, the two glasses have distinct rates of ^{23}Na spin-echo decay (Figure 10b). Because the Mo-0.8 glass is not phase-separated, the decay rate may be taken to be characteristic of Na^+ ions homogeneously distributed throughout these types of borosilicate glasses. The faster decay of the Mo-1.7 glass must be due to the presence of additional dipolar interactions. Because the Na^+ cations are not closer to the ^{11}B atoms in this glass than in Mo-0.8 (see ^{11}B{^{23}Na} REDOR section) and since there are no other abundant spin-active nuclei, the difference between the two glasses very likely indicates clustering of Na^+ cations. This observation is consistent with the known tendency of Mo-bearing glasses to phase-separate and form crystalline molybdates.[57] Scanning electron microscopy images of such materials reveal spherical Na_2MoO_4 inclusions, their shape indicating the occurrence of liquid−liquid phase separation prior to crystallization.[54] While no crystallization is observed in the present case, Na clustering within a Mo-rich phase would produce the ^{23}Na NMR data shown here for the Mo-rich glass, and is also consistent with the slight measured increase in Si-Q^4 with respect to Si-$Q^{3/2}$ in Mo-1.7. This also indicates that the first step in the phase−separation process is the migration of the Na^+ cations (and not the Cs^+) from the borosilicate glassy matrix to the molybdate-rich phase.

3.4. Phase Separation in Mo-Bearing Borosilicate Glasses. Taken together, the NMR results present a clear and consistent picture of the phase segregation processes that appear to be occurring in these two materials.

For the 0.8 mol % MoO_3 glass, the high degree of Si−B mixing observed by ^{11}B−^{29}Si NMR indicates that it is not phase-separated, and various double-resonance and spin−echo curves show a homogeneous distribution of the cations within the borosilicate network with no evidence of crystalline molybdate formation. This implies that in the high-temperature melt, molybdate anions are located in alkali-rich interstices within the network,

(61) Gee, B.; Eckert, H. *Solid State Nucl. Magn. Reson.* **1995**, *5*, 113–122.
(62) Ratai, E.; Janssen, M.; Eckert, H. *Solid State Ionics* **1998**, *105*, 25–37.

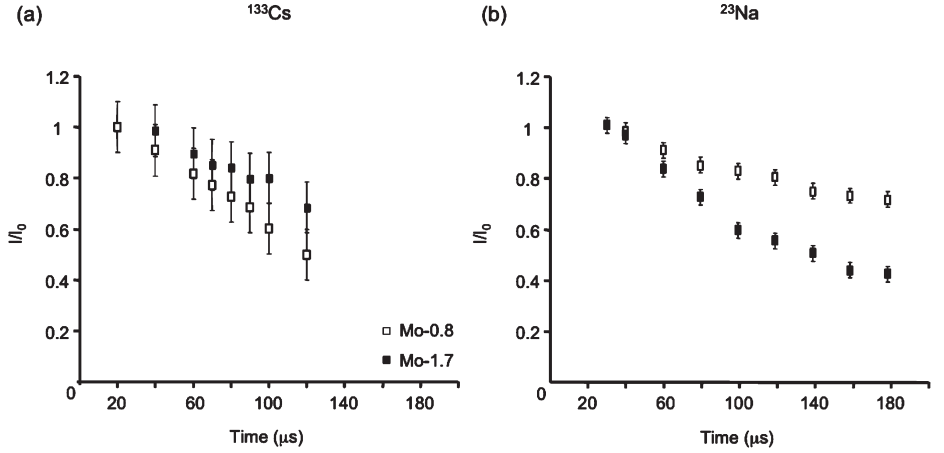

Figure 10. (a) ^{133}Cs and (b) ^{23}Na static spin−echo intensity decay for the two borosilicate glasses under study.

but are of insufficient concentration to form clusters of appreciable size.

For the 1.7 mol % MoO_3 glass, ^{23}Na NMR results show clustering of the Na^+ cations, very likely around the molybdate units, which could lead to the sodium molybdate formation observed in higher Mo-content glasses. In fact, slow quenching a liquid of identical composition resulted in the crystallization of sodium molybdate.[57] On the contrary, the Cs^+ cations do not seem to be influenced by the molybdenum content, suggesting that the Cs^+ ions are distributed within the borosilicate network(s) rather than in the alkali-rich regions. This study therefore suggests that Na^+ cations are the first cations to migrate from the borosilicate matrix to the stable alkali-molybdate phase during the phase-separation process prior to the precipitation of the crystalline molybdate phases.

However, the macroscopic structural changes implied by the NMR data go substantially beyond the direct effects of molybdate clustering. $^{29}Si-^{11}B$ double resonance NMR experiments of the glass reveal a decrease in B−Si network mixing, indicating some degree of separation into a silicon-rich phase−probably enriched in Si-Q^4 and BO_3 units−and a boron-rich phase with a higher level of anionic BO_4 units. Such a scenario is reminiscent of metastable liquid−liquid immiscibility, long known to occur in certain regions of the sodium borosilicate phase diagram.[63] If the composition of these glasses is projected onto a generic ternary alkali-borosilicate phase diagram, it falls just outside the general liquid−liquid immiscibility region. With the migration of alkali ions into the putative molybdate-rich regions of the melt, the composition of the (homogeneous) borosilicate liquid becomes slightly depleted in alkali ions, and shifts in the direction of the immiscibility region. Upon quenching, this compositional shift appears to be sufficient to stimulate metastable liquid−liquid immiscibility, resulting in silicate- and borate-rich phases which are detected by NMR. Hence, the NMR measurements provide evidence of three distinct glassy phases, and two phase-separation mechanisms.

(63) Du, L.-S.; Stebbins, J. F. *J. Phys. Chem. B* **2003**, *107*, 10063–10076.

4. Conclusions

Double-resonance NMR experiments have been used in conjunction with multinuclear single-resonance NMR experiments to probe liquid−liquid phase separation in molybdenum-bearing borosilicate glasses. We have shown that by implementing a CPMG pulse-train during the acquisition period of the usual REDOR experiments, double-resonance experiments involving ^{29}Si in natural abundance can be acquired in a reasonable amount of time. While the single-resonance NMR results are similar and report principally on the short-range order, the double-resonance NMR results for the two glasses are distinct and correlate with their homogeneous or heterogeneous nature. Taken together, the NMR results present a clear and consistent picture of the phase segregation processes that appear to be occurring in these two materials. This work also highlights the potential of double-resonance NMR techniques to probe liquid−liquid phase-separation phenomena by yielding additional structural details, in particular on the composition of the different phases, which are exceedingly difficult to obtain by other physicochemical techniques.

Acknowledgment. S.K. is grateful to NSERC of Canada and the Canada Foundation for Innovation for ongoing financial support. V.K.M. acknowledges an NSERC postgraduate scholarship. The authors thank Chuck Mullen (Varian, Inc.) for his assistance in special probe tunings. We also thank an anonymous reviewer for insightful comments that strengthened this report.